

Remanent magnetic configurations in cylindrical nanodots

R. Moreno¹ and P. G. Bercoff^{1,2}

¹*Instituto de Física Enrique Gaviola, IFEG (UNC-CONICET), Medina Allende s/n, Ciudad Universitaria, 5000 Córdoba, Argentina*

²*Facultad de Matemática, Astronomía, Física y Computación, Universidad Nacional de Córdoba, Argentina.*

(*Electronic mail: rmoreno@conicet.gov.ar)

Determining whether the magnetization of cylindrical nanodots is in a single domain configuration (SD) or a vortex state V_X is crucial in a wide range of interdisciplinary applications. In this work we investigate the SD and V_X existence, and their coexistence, in terms of the nanodot diameter (D) and its saturation magnetization (M_S) for different thicknesses, by means of micromagnetic simulations. We determine the stable magnetic configurations at remanence, from both in plane and out of plane hysteresis loops. Additionally, we investigate the vortex core radius R_V in terms of different parameters considered. We find that R_V is strongly dependent on the thickness and the saturation magnetization but the dependence is weaker on the diameter, vanishing for the larger ones. For the range of parameters studied in this work, we find that R_V is diameter independent for $D \gtrsim 100$ nm.

I. INTRODUCTION

Efforts to master nanomagnetism have been ongoing for some time due to the intriguing properties exhibited by magnets at the nanoscale, which open the door to the possibility of functionalizing their magnetic response to different external stimuli in terms of their shape and size. The specific case of magnetic nanodots, particularly those with cylindrical symmetry, is of special interest due to their potential applications in interdisciplinary research fields.

In these nanostructures, the competition between exchange energy and magnetostatic energy gives rise to two very different types of magnetic domain states: the single domain configuration (SD)¹, in which the magnetization of the system behaves as a single macrospin; and the vortex state (V_X), in which the magnetization curls circularly in plane but smoothly gets out of plane towards the center of the vortex where it points perpendicularly^{2,3}. The distance that takes the magnetization to get from the out of plane configuration (center of the vortex) to the in-plane configuration is defined as the V_X radius (R_V).

Prior knowledge of the nanodot domain state is crucial for most applications. For instance, SD nanodots are desirable for ultra high density magnetic recording devices to avoid the signal-to-noise ratio when reducing the bit size to the nanoscale^{4,5}. Contrarily, nanodots with a V_X configuration have been proposed for nano oscillators due to the gyrotropic motion this soliton presents under the action of constant external stimulus^{6,7}. The domain state in magnetic nanodots is also of special relevance for magnetic random access memory (MRAM) applications⁸. In biomedicine, it has been demonstrated that nanodots within a V_X state are capable of destroying cancer cells by the mechanical torque induced by an external oscillating magnetic field⁹. Furthermore, they are effective nanostructures for producing magnetic hyperthermia, outperforming smaller nanodisks exhibiting SD configurations¹⁰. In paleomagnetism, oblate-like nanoparticles mimicking cylindrical nanodots have been observed in natural samples such as meteorites¹¹ and the question of whether these structures are in a SD or V_X state becomes relevant¹²⁻¹⁴ as they are not

expected to have the same recording fidelity of ancient magnetic fields¹⁵.

The occurrence of a SD configuration or a V_X state in a nanodot depends primarily on its geometrical dimensions and the magnetic material composition. This is in analogy with the type of magnetic domain wall (DW) hosted in cylindrical nanowires¹⁶. Based on general knowledge of nanomagnetism, SD configurations are expected in very small nanodots as well as in either very prolate or very oblate nanodots. Magnetic materials, whose saturation magnetization value M_S is low favor the SD configuration while harder materials —whose M_S value is high— produce magnetization curling and consequently a V_X state. This has been demonstrated by means of different analytical approaches¹⁷⁻¹⁹, yielding phase maps delimiting the existence of the V_X and SD in terms of the nanodot diameter D and thickness T .

In analytical calculations, nanodot geometrical parameters are often normalized by the exchange length to include the influence of the nanodot composition. Computational micromagnetism has corroborated analytical predictions, showing agreement in soft magnetic materials such as permalloy²⁰ or magnetite²¹. Additionally, there exist experimental results confirming previous assessments²²⁻²⁵. However, there is still a gap to bridge for materials with high M_S where the stronger magnetostatic energy coming from the high M_S may lead to a more complex magnetic behavior, not necessarily matching analytical predictions. For instance, it could happen that V_X states are not fully developed, i.e., curling occurs but magnetization does not reach an in-plane configuration, thus leading to magnetic charges in the surfaces which are often neglected in analytical calculations. To the best of our knowledge, numerical studies on these systems are scarce and a systematic study considering the effect of varying M_S is missing.

Another point which is often neglected in the literature is the influence of these parameters on the R_V value. In analogy with DW dynamical behavior in magnetic nanowires, which is strongly influenced by the DW width (δ_w), the vortex radius R_V has a significant contribution to the V_X dynamical behavior²⁶. Moreover, R_V is an important parameter that determines the stability and switching behavior of V_X domain states³. Thus, gaining insights on the dependence of R_V in

terms of the nanodot composition and its geometry will contribute to the optimal nanodot functionalization. R_V values are found to range between 10 nm and 30 nm^{27–29} for magnetic nanodots composed of soft materials such as permalloy. Nevertheless, there exists a lack of studies in the literature in which a systematic study of the possible parameters influencing the R_V size and composition are considered, except for the analytical work done by Metlov³⁰.

In this work we aim to fill these gaps of knowledge. By means of micromagnetic simulations, we extend the existing insight on how the magnetostatic energy influences the V_X state. Specifically, we consider a wide range of nanodot thicknesses and diameters, and for each one, we determine the existence, or coexistence, of the SD and the V_X state in terms of its saturation magnetization value. Using the comprehensive set of numerical models for remanent states in which we have obtained the vortex state, we determine the vortex radius dependence on the nanodot geometry and its saturation magnetization. Results are compared with existing theories for the vortex radius.

II. MODEL

Numerical models have been created using the open-source software package MERRILL³¹, which is a three-dimensional finite-element micromagnetic modeling application. Nanodot geometries are defined in terms of a finite element mesh, which were generated using the open source 3D finite element mesh generator Gmsh³². A 2 nm discretization length was chosen to ensure it is smaller than the exchange length (l_{exc}) corresponding to the highest saturation magnetization material, with this value being ~ 2.1 nm. The diameter and thickness characterizing the set of nanodots studied in this work range from $D = 20$ nm to $D = 200$ nm, and $T = 10$ nm to $T = 50$ nm, respectively.

MERRILL takes into account the exchange, the magnetostatic, the magneto-crystalline and the Zeeman energies. The magnetization configuration is determined by minimizing the total magnetic energy of the system. The minimization is performed using the conjugate gradient algorithm, which adjusts the magnetic moments iteratively until the system reaches an equilibrium state where the total energy is minimized. The exchange stiffness used in this work is a typical value suitable for permalloy $A = 1 \cdot 10^{-11}$ J/m. For simplicity, we do not vary A in our simulations. The saturation magnetization is considered a free parameter, specifically, $\mu_0 M_S$ ranges from 0.6 to 2.4 T. In this study, we include high M_S values in order to capture the behavior of materials such as FeCo alloys³³. Finally, no magnetocrystalline anisotropy energy has been considered in order to simplify the study of the role that magnetostatic energy plays in the magnetic configurations addressed at remanence.

We additionally use the NMAG micromagnetic code³⁴ to corroborate MERRILL results. Notice that MERRILL is a micromagnetic code scoped for research in paleomagnetism and it is barely used in the Materials Science community. Thus, we decided to use NMAG, that works using finite el-

ements as well as MERRILL does, but integrates the LLG equation instead of performing energy minimization to address states of local energy minima. We have reproduced the 20 nm case, obtaining a good agreement between both codes.

We have created numerical models for the hysteretic response of all different geometries and M_S values for both in-plane (IP) and out-of-plane (OoP) applied magnetic field. For these hysteresis loop simulations, we use static energy minimization, so there is no explicit time-stepping or integration scheme involved, as would be the case in dynamic simulations. At each external field step in the hysteresis loop simulation, the system is allowed to relax to an equilibrium configuration before moving to the next field step. The system is considered at equilibrium when the change in energy or magnetization between iterations is below a specified threshold. The maximum applied field values are 0.2 T and 1 T for the IP and OoP cases, respectively. Their corresponding field steps are 0.005 T and 0.01 T, respectively. Simulations started with the magnetization saturated in the direction in which the magnetic field is applied. Within this range of applied fields the magnetization remains saturated for the highest field strength in most of the cases considered in this work.

The magnetic configuration in a V_X state is cylindrically symmetric but height dependent²⁰, thus R_V is too. We average the magnetization in the height and azimuthal dimensions yielding a magnetization that only depends on the radial dimension. The value of R_V presented in this work is obtained from the average normalized magnetization in terms of the distance from the centre of the V_X , i.e. $m(r)$. We determine the distance at which the OoP component vanishes, following this widely accepted criterion in the literature^{27,28}. The cases in which curling occurs but magnetization does not reach the IP configuration because the nanodot radius is not large enough, are obviated for the definition of the R_V value but are considered as V_X states.

III. RESULTS

The only solutions found in our numerical models at remanence are the two widely reported magnetic configurations exhibited in magnetic nanodots: the SD and the V_X states. However, the direction in which the SD and the V_X core point is different depending on the geometry, the composition (defined by the M_S value) and the external magnetic field orientation. Both SD and V_X states can be either parallel or perpendicular to the nanodot c axis. Illustrations of the magnetic distributions of the IP and OoP V_X states obtained for different parameters are presented in Fig. 1.

Figure 2 summarizes the different domain states, obtained for both the IP and OoP magnetic field set ups, displayed in phase diagrams. Specifically, for each M_S and D case, we represent the two equilibrium magnetic configurations found from the IP and the OoP hysteresis. These could be equal or different (coexistence of domain states). In this figure we present the results obtained for two representative thicknesses (20 nm and 30 nm). We additionally include the analytical expression obtained in Hoffmann et al.¹⁷, $\mu_0 M_S =$

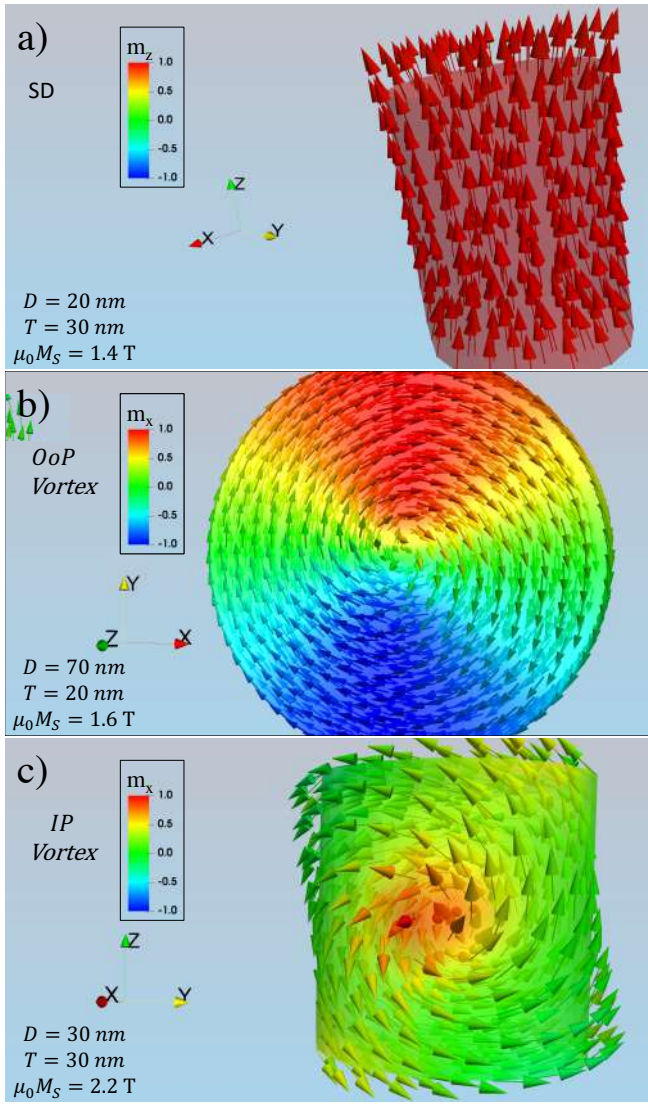


FIG. 1. Spatial distribution representations of the magnetization for the single domain case with the magnetization pointing parallel to the nanodot axis and the two types of V_X states found in this work: a) SD, b) OoP vortex and c) IP vortex. The specific parameters used in each case are described in the corresponding figure.

$\sqrt{\frac{64A}{\pi TD}(\ln(D/2a) + \gamma)}$ with a dashed line to compare with our numerical results (symbols). Here a means the atomic lattice parameter, which has been considered a constant value in terms of M_S with a typical value of 3 \AA . The parameter $\gamma \approx 0.577$ is the Euler's constant. The analytical equation delimits which domain state has lower energy: the SD is the energy minimum below the dashed line while the V_X state is the minimum above it. This expression cannot however discriminate their coexistence. Despite some important approximations done on derivation of this expression¹⁷, such as the cubic lattice assumption or the omission of the vortex core in the energy calculation, it fairly agrees with our full numerical simulations, especially for oblate like cases.

The SD configuration is not discriminated in Fig. 2 be-

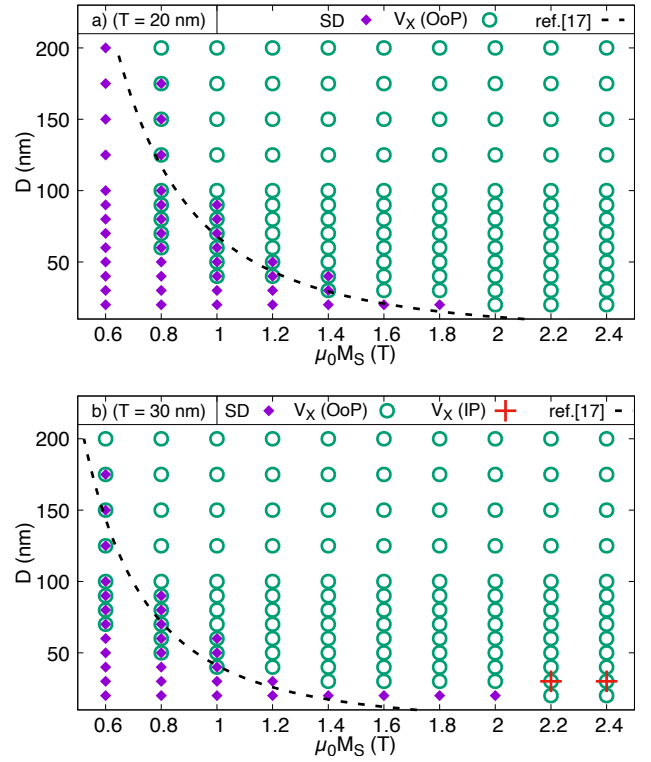


FIG. 2. Phase diagram of magnetic configurations for two different nanodot thicknesses, in terms of their diameter and saturation magnetization. a) and b) correspond to $T = 20 \text{ nm}$ and $T = 30 \text{ nm}$ respectively. Full diamonds, open circles and crosses represent single domain, OoP vortex state and IP vortex, respectively.

tween the IP and the OoP orientations. Contrarily, the presence of IP and OoP V_X states is explicitly clarified. This is to briefly highlight the IP V_X configuration, as it is a rarely found configuration in our numerical models as well as a poorly reported domain state in the literature, albeit with few exceptions, e.g., the work of Ha et al.²⁰. From the few examples found in our work, we suggest that IP V_X prefers to appear in equidimensional nanodots, as depicted in Fig. 1c. The larger the equidimensional nanodot, the lower M_S is required to produced this state²⁰. It should be noticed that this configuration does not exhibit an antivortex pair, contrarily to what happens in the vortex-antivortex domain wall (VAV_{dw}) in cylindrical nanowires, in which the antivortex state appears always together with the vortex one in either wide cylindrical cross sections or nanowires with high M_S ^{16,35}. Elongation makes the difference between these two cylindrical symmetric nanostructures.

Figure 2 indicates that the thicker the nanodot, the more extensive the V_X domain state region is. It is worth mentioning that the V_X state for some of the studied parameters depends on the magnetic field setup (coexistence region). OoP hysteresis favors obtaining the V_X state rather than the IP one. Additionally, Fig. 2 shows that nanodots composed of materials with high M_S values strongly favor the V_X state, even for very small nanodot diameters. Consequently, the vortex core must

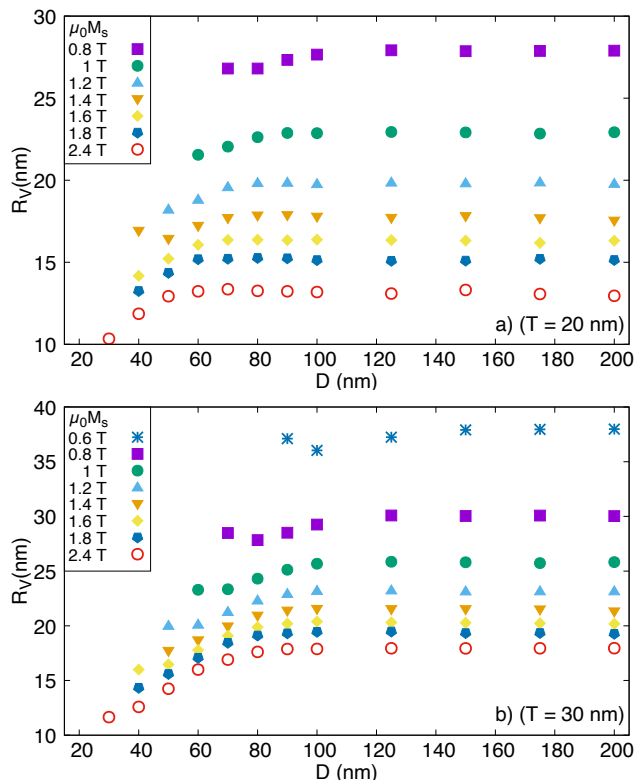


FIG. 3. Vortex radii in terms of the diameter for different saturation magnetization values, for two nanodot thicknesses: a) $T = 20$ nm and b) $T = 30$ nm. M_S values are depicted with different symbols and colors. Some cases for high M_S are not shown to avoid overlapping and simplify visualization. Some R_V values which appear as vortices in Fig. 2 are not displayed here because, despite curling occurs, magnetization does not reach an in plane configuration, thus we cannot determine R_V for these cases.

be very narrow too. The set of V_X radii obtained from our calculations are summarized in Fig. 3 for the same nanodot thicknesses presented before. We remark that Fig. 3 presents the results for the radius of the OoP V_X states independently if they are found either in the OoP or the IP hysteretic configuration, or in both. For the latter case, the R_V is the same.

It should be emphasized that there are domain states defined as V_X in Fig. 2 without their corresponding R_V presented in Fig. 3. This happens regularly for small nanodot diameters at each M_S case. The reason is that in these cases, curling clearly occurs but the magnetization does not reach the in plane configuration within the nanodot nanostructure, i.e., R_V is larger than the nanodot radius. For each M_S , we regularly observe a slight decrease of R_V in terms of the diameter for the smallest value, continued by a change of trend which shows a rapid increase in R_V . This could be attributed to surface effects, as the vortex core is comparable to the nanodot diameter. Indeed, this increase rate drastically slows down and R_V reaches a rather constant value at large enough diameters, varying only a few Angstroms.

The vortex radii of the larger diameters are assessed considering the corresponding R_V value for each M_S and nanodot

thickness. The set of calculated R_V values is illustrated in Fig. 4 as a function of the saturation magnetization (Fig. 4a) and in terms of the nanodot thickness (Fig. 4b). Different experimental data points extracted from the literature have been included in Fig. 4a, showing good agreement with the calculations. Additionally, analytical expressions reported in the literature for R_V (solid lines) are also depicted in the figures for comparison. The first (displayed in Fig. 4a) corresponds to the typical domain wall width of a 180° Bloch domain wall, $\delta_W = \pi\sqrt{2A/\mu_0 N_Z M_S^2}$, where μ_0 is the vacuum permeability and $N_Z = 1$ is the demagnetizing factor for an infinite oblate nanodot. The curve plotted in Fig. 4b corresponds to the analytical expression for R_V derived by K. Metlov³⁰.

On the one hand, good qualitative agreement is obtained between the numerical and analytical results in Fig. 4a. This implies that $R_V \sim 1/M_S$. Moreover, also good quantitative agreement is observed, as R_V approximates the analytical expression for the most oblate nanodot case considered in this work. However, on the other hand, the analytical expression plotted in Fig. 4b does not follow our numerical calculations either quantitatively nor –more importantly– qualitatively. This curve, corresponding to Metlov’s work³⁰, has been calculated using the value $\mu_0 M_S = 2.4$ T, with a corresponding exchange length of $l_{exc} = \sqrt{2A/\mu_0 M_S^2} = 2.1$ nm. A different M_S will not change its trend, but just its magnitude, showing that additional considerations should be made in the models to achieve a better correlation between them.

IV. CONCLUSION

We report a systematic study on the possible domain states presented in cylindrical magnetic nanodots at remanence, by means of micromagnetic simulations. We have focused on the OoP V_X domain state and, in particular, we have determined the vortex core radius in terms of the geometry and saturation magnetization. Also, a comparison with different analytical approaches found in the literature has been carried out.

We have verified that the expression derived by Hoffmann et al.¹⁷ is robust enough, compared with our full micromagnetic simulations, to determine whether a SD or a V_X state will be exhibited by an experimental nanodot, characterized by a given geometry and composition. However, this expression does not account for coexistence of the different domain states. We show that either slightly below and above of the limit that this expression establishes, the existence of SD and V_X states could be promoted by the particular field orientation; specifically the SD and V_X are favored by the IP and OoP field directions, respectively.

We have determined the vortex core radius for each case considered in this work, verifying the established $R_V(M_S) \sim 1/M_S$ dependence. Furthermore, we showed good quantitative agreement for more oblate geometries. Contrarily, we find that the R_V thickness dependence is not properly described by the analytical models currently available in the literature. While theoretical calculations predict a logarithmic dependence of R_V on the thickness, our results indicate it seems to

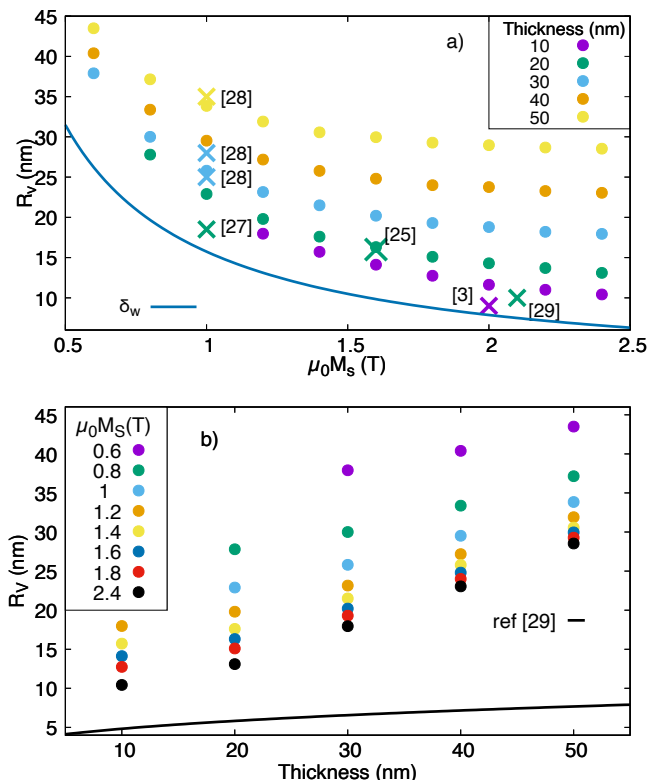


FIG. 4. a) Vortex radii obtained for large diameters in terms of M_S for various thickness values. The solid line represents the analytical value of the domain wall width for an ideal oblate nanodisk. Different R_V values found in the literature are also displayed with crosses and their corresponding reference number. The crosses color indicates the thickness of these dots. b) Vortex radii as a function of thickness for various M_S values. The solid line corresponds to the analytical expression given in ref.²⁹

be linear for thickness values above 20 nm, or even parabolic if considering the lower thicknesses.

In conclusion, we presented a numerical study bridging different gaps of knowledge in magnetic nanodots. We aim that this results will leverage the functionalization of magnetic nanodots for different interdisciplinary applications.

ACKNOWLEDGMENTS

This work used computational resources from CCAD-UNC, which is part of SNCAD-MinCyT, Argentina. R. M. acknowledges a postdoctoral fellowship from Conicet, Argentina. This work has been partially funded by Secyt-UNC, ANPCyT-FONCyT and Conicet (Argentina).

DATA AND CODE AVAILABILITY

The data that support the findings of this study are available from the corresponding author upon reasonable request. The results can be reproduced using the data found in the

manuscript. Geometry meshes were generated using Gmsh³². Micromagnetic models have been created using MERRILL³¹ and NMAG³⁴.

AUTHOR CONTRIBUTIONS

Roberto Moreno: Writing – original draft, Validation, Methodology, Formal analysis, Data curation, Conceptualization. Paula G. Bercoff: Writing – review & editing, Project administration, Methodology, Formal analysis.

DECLARATIONS

A. Conflict of interest

The authors declare no conflicts of interest related to this study.

B. Ethical approval

Not applicable

REFERENCES

- E. W. Lee and J. E. L. Bishop, “Magnetic behaviour of single-domain particles,” *Proceedings of the Physical Society* **89**, 661 (1966).
- T. Shinjo, T. Okuno, R. Hassdorf, K. Shigeto, and T. Ono, “Magnetic vortex core observation in circular dots of permalloy,” *Science* **289**, 930–932 (2000), <https://www.science.org/doi/pdf/10.1126/science.289.5481.930>.
- A. Wachowiak, J. Wiebe, M. Bode, O. Pietzsch, M. Morgenstern, and R. Wiesendanger, “Direct observation of internal spin structure of magnetic vortex cores,” *Science* **298**, 577–580 (2002), <https://www.science.org/doi/pdf/10.1126/science.1075302>.
- B. D. Terris, L. Folks, D. Weller, J. E. E. Baglin, A. J. Kellock, H. Rothuizen, and P. Vettiger, “Ion-beam patterning of magnetic films using stencil masks,” *Applied Physics Letters* **75**, 403–405 (1999), https://pubs.aip.org/aip/apl/article-pdf/75/3/403/18542943/403_1_online.pdf.
- C. Ross, “Patterned magnetic recording media,” *Annual Review of Materials Research* **31**, 203–235 (2001).
- G. Hrkac, P. S. Keatley, M. T. Bryan, and K. Butler, “Magnetic vortex oscillators,” *Journal of Physics D: Applied Physics* **48**, 453001 (2015).
- E. Grimaldi, R. Lebrun, A. Jenkins, A. Dussaux, J. Grollier, V. Cros, A. Fert, H. Kubota, K. Yakushiji, A. Fukushima, R. Matsumoto, S. Yuasa, G. Cibiel, P. Bortolotti, and G. Pillet, “Spintronic nano-oscillators: Towards nanoscale and tunable frequency devices,” in *2014 IEEE International Frequency Control Symposium (FCS)* (2014) pp. 1–6.
- A. Meo, P. Chureemart, S. Wang, R. Chepulskyy, D. Apalkov, R. W. Chantrell, and R. F. L. Evans, “Thermally nucleated magnetic reversal in cofeb/mgo nanodots,” *Scientific Reports* **7**, 16729 (2017).
- D.-H. Kim, E. A. Rozhkova, I. V. Ulasov, S. D. Bader, T. Rajh, M. S. Lesniak, and V. Novosad, “Biofunctionalized magnetic-vortex microdiscs for targeted cancer-cell destruction,” *Nature Materials* **9**, 165–171 (2010).
- Z. Nemati, S. Salili, J. Alonso, A. Ataie, R. Das, M. Phan, and H. Srikanth, “Superparamagnetic iron oxide nanodiscs for hyperthermia therapy: Does size matter?” *Journal of Alloys and Compounds* **714**, 709–714 (2017).
- J. F. Einsle, R. J. Harrison, T. Kasama, P. O. Conbhui, K. Fabian, W. Williams, L. Woodland, R. R. Fu, B. P. Weiss, and P. A. Midgley, “Multi-scale three-dimensional characterization of iron particles in dusty

- olivine: Implications for paleomagnetism of chondritic meteorites,” *American Mineralogist* **101**, 2070–2084 (2016).
- ¹²L. Nagy, R. Moreno, A. R. Muxworthy, W. Williams, G. A. Paterson, L. Tauxe, and M. A. Valdez-Grijalva, “Micromagnetic determination of the FORC response of paleomagnetically significant magnetite assemblages,” *Geochemistry, Geophysics, Geosystems* **25**, e2024GC011465 (2024), e2024GC011465 2024GC011465, <https://agupubs.onlinelibrary.wiley.com/doi/pdf/10.1029/2024GC011465>.
- ¹³W. Williams, R. Moreno, A. R. Muxworthy, G. A. Paterson, L. Nagy, L. Tauxe, U. Donardelli Bellon, A. A. Cowan, and I. Ferreira, “Vortex magnetic domain state behavior in the day plot,” *Geochemistry, Geophysics, Geosystems* **25**, e2024GC011462 (2024), e2024GC011462 2024GC011462, <https://agupubs.onlinelibrary.wiley.com/doi/pdf/10.1029/2024GC011462>.
- ¹⁴G. A. Paterson, R. Moreno, A. R. Muxworthy, L. Nagy, W. Williams, and L. Tauxe, “Magnetic hysteresis properties of magnetite: Trends with particle size and shape,” *Geochemistry, Geophysics, Geosystems* **25**, e2024GC011461 (2024), e2024GC011461 2024GC011461, <https://agupubs.onlinelibrary.wiley.com/doi/pdf/10.1029/2024GC011461>.
- ¹⁵L. Nagy, W. Williams, A. R. Muxworthy, K. Fabian, T. P. Almeida, P. O. Conbhuf, and V. P. Shcherbakov, “Stability of equidimensional pseudo-single-domain magnetite over billion-year timescales,” *Proc. Nat. Acad. Sci. U.S.A.* **114**, 10356–10360 (2017).
- ¹⁶R. Moreno, V. Carvalho-Santos, D. Altbir, and O. Chubykalo-Fesenko, “Detailed examination of domain wall types, their widths and critical diameters in cylindrical magnetic nanowires,” *J. Magn. Mag. Mat.* **542**, 168495 (2022).
- ¹⁷H. Hoffmann and F. Steinbauer, “Single domain and vortex state in ferromagnetic circular nanodots,” *Journal of Applied Physics* **92**, 5463–5467 (2002), https://pubs.aip.org/aip/jap/article-pdf/92/9/5463/19128438/5463_1_online.pdf.
- ¹⁸P.-O. Jubert and R. Allenspach, “Analytical approach to the single-domain-to-vortex transition in small magnetic disks,” *Phys. Rev. B* **70**, 144402 (2004).
- ¹⁹K. L. Metlov and K. Y. Guslienko, “Stability of magnetic vortex in soft magnetic nano-sized circular cylinder,” *Journal of Magnetism and Magnetic Materials* **242-245**, 1015–1017 (2002), proceedings of the Joint European Magnetic Symposia (JEMS’01).
- ²⁰J. K. Ha, R. Hertel, and J. Kirschner, “Micromagnetic study of magnetic configurations in submicron permalloy disks,” *Phys. Rev. B* **67**, 224432 (2003).
- ²¹D. Gregurec, A. W. Senko, A. Chuvilin, P. D. Reddy, A. Sankararaman, D. Rosenfeld, P.-H. Chiang, F. Garcia, I. Tafel, G. Varnavides, E. Cio-can, and P. Anikeeva, “Magnetic vortex nanodiscs enable remote magnetomechanical neural stimulation,” *ACS Nano* **14**, 8036–8045 (2020), pMID: 32559057, <https://doi.org/10.1021/acsnano.0c00562>.
- ²²C. A. Ross, M. Hwang, M. Shima, J. Y. Cheng, M. Farhoud, T. A. Savas, H. I. Smith, W. Schwarzacher, F. M. Ross, M. Redjald, and F. B. Humphrey, “Micromagnetic behavior of electrodeposited cylinder arrays,” *Phys. Rev. B* **65**, 144417 (2002).
- ²³S.-H. Chung, R. D. McMichael, D. T. Pierce, and J. Unguris, “Phase diagram of magnetic nanodisks measured by scanning electron microscopy with polarization analysis,” *Phys. Rev. B* **81**, 024410 (2010).
- ²⁴R. P. Cowburn, D. K. Koltsov, A. O. Adeyeye, M. E. Welland, and D. M. Tricker, “Single-domain circular nanomagnets,” *Phys. Rev. Lett.* **83**, 1042–1045 (1999).
- ²⁵J. Mejía-López, D. Altbir, P. Landeros, J. Escrig, A. H. Romero, I. V. Roshchin, C.-P. Li, M. R. Fitzsimmons, X. Batlle, and I. K. Schuller, “Development of vortex state in circular magnetic nanodots: Theory and experiment,” *Phys. Rev. B* **81**, 184417 (2010).
- ²⁶S.-B. Choe, Y. Acremann, A. Scholl, A. Bauer, A. Doran, J. Stöhr, and H. A. Padmore, “Vortex core-driven magnetization dynamics,” *Science* **304**, 420–422 (2004), <https://www.science.org/doi/pdf/10.1126/science.1095068>.
- ²⁷W. Scholz, K. Guslienko, V. Novosad, D. Suess, T. Schrefl, R. Chantrell, and J. Fidler, “Transition from single-domain to vortex state in soft magnetic cylindrical nanodots,” *Journal of Magnetism and Magnetic Materials* **266**, 155–163 (2003), proceedings of the 4th International Conference on Fine Particle Magnetism (ICFPM).
- ²⁸M. Goiriena-Goikoetxea, K. Y. Guslienko, M. Rouco, I. Orue, E. Berganza, M. Jaafar, A. Asenjo, M. L. Fernández-Gubieda, L. Fernández Barquín, and A. García-Arribas, “Magnetization reversal in circular vortex dots of small radius,” *Nanoscale* **9**, 11269–11278 (2017).
- ²⁹I. V. Roshchin, C.-P. Li, H. Suhl, X. Batlle, S. Roy, S. K. Sinha, S. Park, R. Pynn, M. R. Fitzsimmons, J. Mejía-López, D. Altbir, A. H. Romero, and I. K. Schuller, “Measurement of the vortex core in sub-100 nm Fe dots using polarized neutron scattering,” *Europhysics Letters* **86**, 67008 (2009).
- ³⁰K. L. Metlov, “Analytical approximations to the core radius and energy of magnetic vortex in thin ferromagnetic disks,” *Journal of Magnetism and Magnetic Materials* **343**, 55–59 (2013).
- ³¹P. O Conbhuf, W. Williams, K. Fabian, P. Ridley, L. Nagy, and A. R. Muxworthy, “Merrill: Micromagnetic earth related robust interpreted language laboratory,” *Geochemistry Geophysics Geosystems* **19**, 1080–1106 (2018), <https://doi.org/10.1002/2017gc007279>.
- ³²C. Geuzaine and J.-F. Remacle, “Gmsh: A 3-d finite element mesh generator with built-in pre- and post-processing facilities,” *International Journal for Numerical Methods in Engineering* **79**, 1309–1331 (2009), <https://onlinelibrary.wiley.com/doi/pdf/10.1002/nme.2579>.
- ³³T. Lamichhane, L. Sethuraman, A. Dalagan, H. Wang, J. Keller, and M. Paranthaman, “Additive manufacturing of soft magnets for electrical machines—a review,” *Materials Today Physics* **15**, 100255 (2020).
- ³⁴T. Fischbacher, M. Franchin, G. Bordignon, and H. Fangohr, “A systematic approach to multiphysics extensions of finite-element-based micromagnetic simulations: Nmag,” *IEEE Transactions on Magnetics* **43**, 2896–2898 (2007).
- ³⁵G. H. R. Bittencourt, V. L. Carvalho-Santos, O. Chubykalo-Fesenko, D. Altbir, and R. Moreno, “Dynamics of chiral domain walls in bent cylindrical magnetic nanowires,” *Journal of Applied Physics* **135**, 063906 (2024).